Acta Crystallographica Section D
Biological Crystallography
ISSN 0907-4449

Effects of crystal twinning on the ability to solve a macromolecular structure using multiwavelength anomalous diffraction

Fan Yang,[a]† Zbigniew Dauter[b] and Alexander Wlodawer[a]*

[a]Protein Structure Section, Macromolecular Crystallography Laboratory, Program in Structural Biology, National Cancer Institute–FCRDC, Frederick, MD 21702, USA, and [b]Synchrotron Radiation Research Section, Macromolecular Crystallography Laboratory, Program in Structural Biology, National Cancer Institute and NSLS, Brookhaven National Laboratory, Building 725A-X9, Upton, NY 11973, USA

† Current address: The Institute for Genomic Research, 9712 Medical Center Drive, Rockville, Maryland 20850, USA.

Correspondence e-mail: wlodawer@ncifcrf.gov

Received 2 February 2000
Accepted 10 May 2000

The crystal structure of gpD, the capsid-stabilizing protein of bacteriophage λ, was solved by multiwavelength anomalous diffraction (MAD) for a selenomethionine (SeMet) derivative of the protein at 1.8 Å resolution, using crystals in space group $P2_1$ [Yang *et al.* (2000), *Nature Struct. Biol.* **7**, 230–237]. Subsequent analysis showed that the crystals of both the original protein and the SeMet derivative were pseudo-merohedrally twinned with a twinning fraction $\simeq 0.36$, owing to the near-identity of the *a* and *c* axes. An analysis of the crystal structure solution is presented and the utility of twinned crystals for solving the structure using MAD and of different phasing strategies is discussed; the results obtained with several software packages are compared.

1. Introduction

In an ideal crystal, all molecules (or, more strictly, all unique structural motifs building up the contents of the asymmetric unit of the crystal) are related to each other by crystallographic symmetry operations. However, in some cases the orientation of two or more crystalline domains may be related by a special operation. This phenomenon is termed crystal twinning and is different from the much more commonly observed phenomenon in which multiple crystals are clustered randomly together. Although twinning frequently occurs in crystals of small inorganic or organic molecules, it is rarely reported in macromolecular crystallography. One of the reasons for this may be that racemic twinning is not possible because biological macromolecules are chiral and always crystallize in non-centrosymmetric (enantiomorphic) space groups. Another reason may be that twinned crystals are routinely discarded in favor of non-twinned ones. This course of action, however, is not always possible.

Merohedral twinning occurs when the crystal lattice has a higher symmetry than that of the crystal Laue symmetry group, as is the case in polar space groups. The diffraction pattern can then be indexed in several permissible but non-equivalent ways, *e.g.* with the polar axis pointing 'up' or 'down'. In merohedrally twinned crystals, the reflections generated by both twin domains coincide perfectly, as required by crystal symmetry. If the coincidence of the reflection profiles is close but not required by the crystal symmetry, the phenomenon is termed pseudo-merohedral twinning. Usually, such twinning is the result of the unit-cell parameters being close to fulfilling the requirements of higher symmetry.

Several protein structures have been solved from twinned crystals by molecular replacement (Ito *et al.*, 1995; Luecke *et al.*, 1998; Valegard *et al.*, 1998; Ban *et al.*, 1999; Breyer *et al.*,

Table 1
Analysis of the quality of the two MAD data sets for gpD collected on two synchrotron beamlines.

Data for only one wavelength are presented; the statistics for other wavelengths are very similar.

NSLS remote long wavelength					APS remote long wavelength				
Reso† (Å)	R_{sym}	Comp‡ (%)	>5σ§ (%)	≥4 times¶ (%)	Reso† (Å)	R_{sym}	Comp‡ (%)	>5σ§ (%)	≥4 times¶ (%)
4.11	0.024	97.3	97.0	85.0	4.00	0.022	98.7	98.3	85.7
3.27	0.024	98.6	98.4	90.7	3.18	0.024	99.2	98.8	88.3
2.86	0.027	98.3	98.3	91.9	2.78	0.030	99.1	98.7	90.0
2.59	0.030	98.2	98.1	93.1	2.52	0.036	98.9	97.7	88.6
2.41	0.032	97.9	97.9	92.5	2.34	0.038	98.7	97.8	90.5
2.27	0.036	97.5	97.2	92.7	2.20	0.042	98.3	97.0	89.4
2.15	0.038	97.4	96.9	91.5	2.09	0.045	98.3	96.5	89.6
2.06	0.042	97.0	96.6	91.8	2.00	0.050	97.8	95.7	89.1
1.98	0.047	96.8	96.5	91.6	1.93	0.065	97.8	93.3	88.7
1.91	0.054	96.7	95.8	90.4	1.86	0.074	97.7	90.8	87.5
1.85	0.059	96.6	95.4	88.0	1.80	0.095	97.3	85.3	78.7
1.8	0.068	73.2	70.9	58.8	1.75	0.116	94.4	64.7	56.9
All	0.030	95.4	94.9	88.2	All	0.034	98.0	92.9	85.3

† The upper limit of the resolution shell. ‡ The completeness of the resolution shell. § The percentage of data whose intensities are larger than 5σ. ¶ The percentage of data that have been observed at least four times (Friedel pairs are treated as equivalent observations).

1999) or isomorphous replacement (Yeates & Rees, 1987; Reynolds *et al.*, 1985). However, to the best of our knowledge, no new protein structure has been previously solved from twinned crystals with the use of the MAD method. Recently, we solved the crystal structure of bacteriophage λ head protein D (gpD) at near-atomic resolution (Yang *et al.*, 2000), using MAD. In the process of refining the initial structural model against the high-resolution data set collected for a wild-type gpD crystal, we found that the crystal was actually twinned. Further analysis showed that the SeMet-gpD crystals used for MAD experiments were also twinned. Thus, without noticing it at the time, we had in fact solved the MAD structure by using twinned crystals. In this paper, we describe the data analysis, the comparison of the MAD-phased electron-density maps from twinned or detwinned data and the quality of the MAD-phased electron-density maps obtained using various structure-determination software for two MAD data sets collected from different crystals of SeMet-gpD on two different synchrotron beamlines.

2. Materials and methods

The preparation of wild-type and SeMet-gpD samples, crystallization of gpD, data collection and structure determination have been described elsewhere (Yang *et al.*, 2000). The structure was initially solved by MAD without realising that the crystals were twinned and only later, when the refinement of the structure against native data proved surprisingly difficult, was the possibility of crystal twinning considered and investigated.

There are several methods for detecting twinning and estimating the twinning ratio α. Twinning has profound effects on the statistics of reflection intensities; the cumulative intensity distribution, $N(z)$, is one of the simplest quantities to test. The theoretical $N(z)$ curve for a single crystal is exponential, whereas that of a twinned crystal is sigmoidal (Rees, 1980). This is caused by a lower percentage of very small and very large amplitudes in the twinned data, resulting from the low probability that in the two overlapped lattices both reflections are simultaneously either very weak or very strong. Yeates (1988, 1997) proposed a robust test for twinning based on the cumulative distribution of the ratio $H = |I_{t1} - I_{t2}|/(I_{t1} + I_{t2})$, which depends linearly on H.

The X-rays scattered from the two twin domains do not interfere and the reflection intensities from both domains contribute to the measured intensity proportionally to the twinning volume ratio α. The diffraction intensities of two reflections related by a twinning operation, measured for a crystal with $\alpha < 0.5$, are therefore

$$I_{t1} = (1 - \alpha)I_{s1} + \alpha I_{s2}, \quad (1)$$

$$I_{t2} = \alpha I_{s1} + (1 - \alpha)I_{s2}, \quad (2)$$

where I_{s1} and I_{s2} are the theoretical intensities contributed by the two single-crystal components (Yeates, 1997). I_{s1} and I_{s2} can then be determined as

$$I_{s1} = [(1 - \alpha)I_{t1} - \alpha I_{t2}]/(1 - 2\alpha), \quad (3)$$

$$I_{s2} = [(1 - \alpha)I_{t2} - \alpha I_{t1}]/(1 - 2\alpha). \quad (4)$$

We used this simple formula to detwin the MAD data, treating both Friedel pairs of each acentric reflection separately. Detwinning of intensities that assumes too high a value of α may lead to negative intensities for some reflections, which is unrealistic.

In our reinvestigation of the gpD diffraction data, we used the program *TRUNCATE* from the *CCP*4 program suite (Collaborative Computational Project, Number 4, 1994) to estimate the presence of twinning (French & Wilson, 1978). The program *SHELXL* (Sheldrick & Schneider, 1997), which we used for the structural refinement, can also be used to refine the twinning ratio. The MAD data, collected at a remote long wavelength, were used to determine the protein structure and the twinning ratio of the SeMet-gpD crystals. To compare the performance of the different software used for the structure determination, we processed the MAD data and calculated the phases using *MADSYS* (Hendrickson, 1991), *MLPHARE* (Collaborative Computational Project, Number 4, 1994), *PHASES* (Furey & Swaminathan, 1995), *SHARP* (La Fortelle & Bricogne, 1999) and *SOLVE* (Terwilliger & Berendzen, 1999). We paid particular attention to ensuring that the data were processed under similar conditions and that the results were as comparable as possible.

3. Results and discussion

3.1. Detection and the type of crystal twinning

The native data used for the final structure refinement were collected to a resolution of 1.1 Å at NSLS beamline X9B. Neither visual inspection of the diffraction images nor the intensity-integration procedure indicated any split of the reflection profiles (Fig. 1). Even reflections near the rotation axis, close to the blind region and having high Lorenz factors, which are most sensitive to any abnormalities, do not show any tendency towards splitting. Our analysis with *HKL*2000 (Otwinowski & Minor, 1997) suggested the possibilities of a *C*-centered orthorhombic lattice (a = 56.02, b = 72.13, c = 69.03 Å) and a primitive monoclinic lattice (a = 45.66, b = 69.03, c = 45.67 Å, β = 104.34°). Clearly, the lattice metric is orthorhombic and the data could be integrated equally well in both cases, since the monoclinic Laue symmetry 2/*m* is a subgroup of the orthorhombic Laue symmetry group *mmm*. However, the true crystal space group is determined by the symmetry of reflection intensities, not by the geometry of the lattice. Merging of the data set at 2.15 Å in the $C222_1$ space group led to an R_{sym} of 0.448, which was much higher than the value of 0.052 in the $P2_1$ space group (the exact choice of the space group was based on systematic absences).

Diffraction data for two different SeMet-gpD crystals were collected to resolutions of 1.8 and 1.75 Å at NSLS beamline X9B and APS beamline 14-BM-D, respectively. The two data sets have similar quality and both were used for phase calculations (Table 1). An initial gpD structural model was built based on the electron-density maps calculated with the MAD phases. Although the initial MAD-phased electron-density maps were not as good as expected, the presence of twinning was not suspected until the refinement of the structural model, which was performed using *CNS* (Brunger *et al.*, 1998). The crystallographic residuals R and R_{free} were lowered to about 25 and 29%, respectively, but could not be reduced any further. Subsequent examination of the intensity statistics clearly indicated pseudo-merohedral twinning of the native data. Analysis of the two independent MAD data sets indicated the same phenomenon, as illustrated for the NSLS data in Fig. 2. The data could not be detwinned using the Merohedral Crystal Twinning Server at the Department of Chemistry and Biochemistry, University of California, Los Angeles (http://www.doe-mbi.ucla.edu/Services/Twinning/), because this server does not automatically detect pseudo-merohedral twinning if the twinning operation does not result from the crystal symmetry.

The Harker section of the anomalous difference Patterson map (Fig. 3), calculated with the original data in the monoclinic space group, shows peaks corresponding to all six Se-atom self-vectors and also one cross-vector between a pair of atoms having the same y coordinate (Table 2). Some of the peaks resulting from the second twin domain are present at a much lower level, at positions related by the twinning operation, *i.e.* the diagonal twofold axis. A test Patterson map was calculated from data simulated for a 50:50 twinning ratio by adding intensities of reflections related by the twinning operation so that the resulting intensities agreed with the $C222_1$ symmetry. This map shows both sets of peaks on the Harker section with equal heights and the map has *mmm* symmetry. There are, however, no significant peaks on the two other potential Harker sections corresponding to the orthorhombic system (data not

Table 2
Refined coordinates and B factors of the Se atoms and peaks on the Harker section ($v = \frac{1}{2}$) of the anomalous difference Patterson map, which are also marked in Fig. 3.

Primed sites correspond to the minor twin component.

(*a*) Coordinates and B factors of Se atoms.

Selenium site	x	y	z	B factor
Se1	0.018	0.678	−0.058	17.7
Se2	0.193	0.453	0.029	10.1
Se3	0.493	0.725	−0.402	22.0
Se4	0.598	0.542	−0.130	12.1
Se5	−0.033	0.455	−0.618	17.9
Se6	0.278	0.328	−0.399	11.9

(*b*) Harker vectors.

Se–Se vector	u	w	Height (σ)
Origin peak	0	0	141.0
Se1–Se1	0.035	0.883	7.3
Se2–Se2	0.385	0.057	8.0
Se3–Se3	0.985	0.196	4.0
Se4–Se4	0.197	0.740	6.3
Se5–Se5	0.934	0.764	4.7
Se6–Se6	0.556	0.203	7.3
Se2–Se6	0.159	0.410	13.0
Se5′–Se5′	0.764	0.934	4.3
Se2′–Se6′	0.410	0.159	2.7

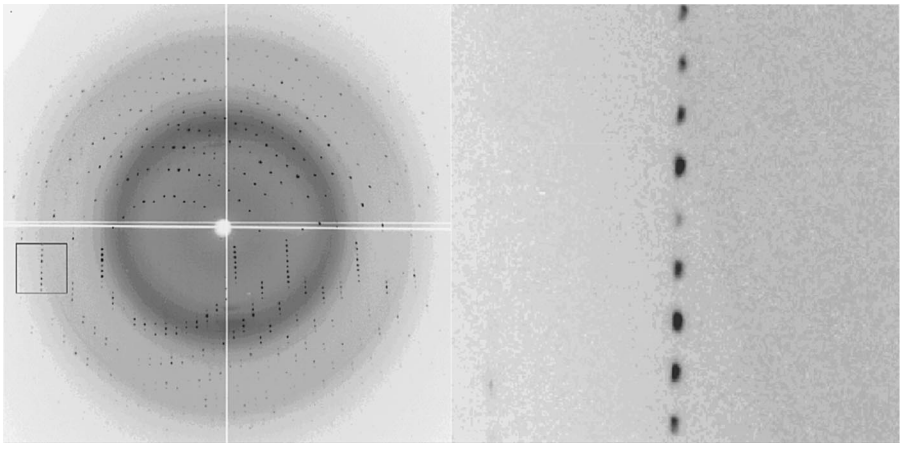

Figure 1
A diffraction pattern of the gpD crystal obtained on beamline X9B at NSLS (Brookhaven National Laboratory). The spot profiles from two twinning domains overlap perfectly and do not show any apparent split. The left image shows a complete frame; the area within the square is shown as an enlargement in the right-hand image.

Table 3
Comparison of electron-density maps calculated from the final refined structural model and those calculated from MAD phases using twinned or detwinned data and various software packages.

Each structure-determination program was used according to the instructions of its authors and to our experience, but no attempt was made to achieve the best performance of any of them. Thus, the comparison of the results should be taken as an indication of their performance under default conditions; we are quite certain that users more experienced with any of them could have obtained better results in their own investigations.

NSLS data			APS data		
	CC (map)†	CC (residue)‡		CC (map)†	CC (residue)‡
MADSYS (detwinned, $\alpha = 0.3$)	0.55	0.81	*MADSYS* (detwinned, $\alpha = 0.3$)	0.51	0.81
MADSYS	0.51	0.76	*MADSYS*	0.48	0.77
SOLVE	0.54	0.82	*SOLVE*	0.50	0.81
SHARP	0.45	0.68	*SHARP*	0.50	0.82
PHASES	0.29	0.42	*PHASES*	0.27	0.45
MLPHARE	0.48	0.58	*MLPHARE*	0.36	0.48

† The correlation coefficients are calculated using all grid points in the map. ‡ The correlation coefficients are calculated based on residues.

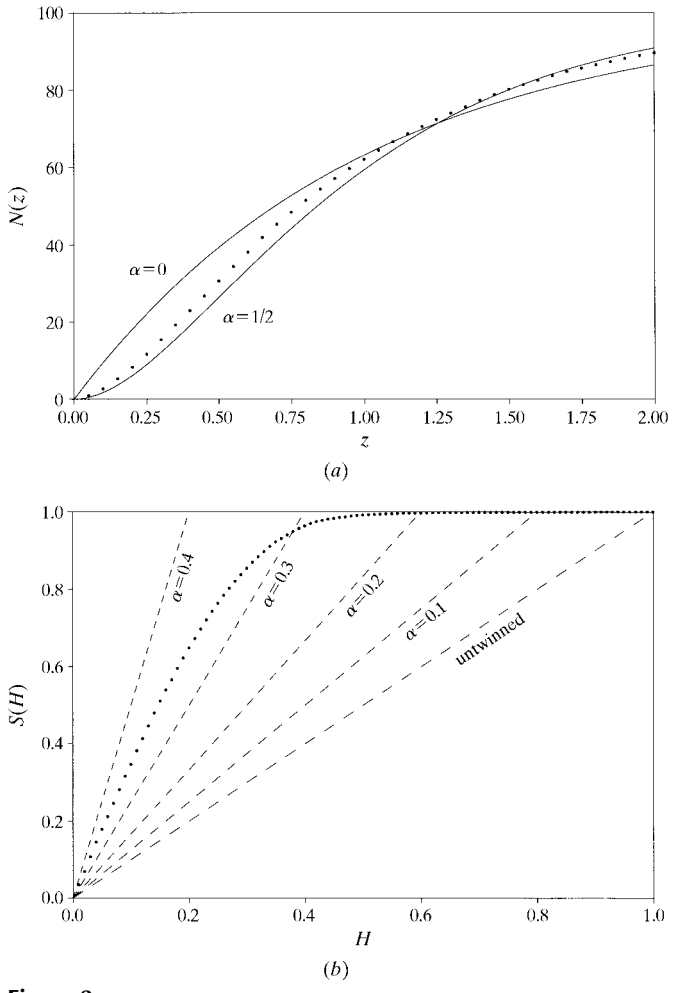

Figure 2
Statistical analysis of the intensities of the twinned data. (*a*) The cumulative distribution of intensities. The experimental distribution for gpD is plotted as a dotted line and the theoretical distributions for perfectly twinned and non-twinned crystals are plotted as solid lines. (*b*) The cumulative distribution of $S(H)$. The experimental distribution for gpD is plotted as a dotted line.

shown). The presence of the 2_1 axis could be therefore identified even if the crystals were perfectly twinned, but the possibility of $C222_1$ crystal symmetry could be excluded by the inspection of all Harker sections.

The crystals of gpD have special unit-cell parameters in that the *a* and *c* axes of the $P2_1$ space group are identical within the error of their estimation. With these results, the twinning operation can be deduced as (001, $0\bar{1}0$, 100), *i.e.* a twofold rotation about the axis diagonal between the monoclinic *a* and *c* directions (it has no relation to the non-crystallographic threefold axis of the trimer that is present in the asymmetric unit). This is analogous to classic merohedral twinning, where the twinning operation can be any symmetry operation existing in the higher (holohedry) symmetry group, but not the lower (merohedry or hemihedry) real symmetry group of the crystal. This assumption was confirmed by a successful refinement of the structure with *SHELXL* (Sheldrick & Schneider, 1997) against the originally measured intensities, refining the twinning ratio using the TWIN and BASF options, which led to the final R and $R_{\rm free}$ of 9.7 and 13.2% at 1.1 Å resolution, respectively (Yang *et al.*, 2000). The twinning ratios of the native data set and the two MAD data sets were refined to 0.362, 0.367 and 0.351 and agree well with the estimation presented in Fig. 2. Thus, if the volume ratio of the two twinned domains was 0.64:0.36, the MAD signal would be less than two-thirds of that of an untwinned crystal. The structure could still be solved owing to the small size of the protein, the stable position of the two Se atoms inside the protein and the high resolution and high quality of the data (Table 1). $R_{\rm sym}$ values for both MAD data sets are in the range 3–3.5% to the resolution of 1.8 or 1.75 Å. A series of tests of correlation coefficients (CC) between the electron-density maps calculated from the structural model and from the MAD phases showed decreased quality with the twinned MAD data at lower resolution (CC of 0.51, 0.46, 0.43, 0.38, 0.36 and 0.34 at the resolution ranges 1.8, 2.1, 2.4, 2.7, 3.0 and 3.3 Å, respectively). Finally, although the twinning ratio seems to be constant in this case, generally it may change by varying the crystallization conditions, an approach often used to overcome the twinning problem.

In general, monoclinic lattices do not support merohedral twinning. In this case, however, the twinning is made possible by the metric symmetry of the lattice and can therefore be termed pseudo-merohedral. The same type of twinning has been reported previously for crystals of deoxyhemoglobin from the Antarctic fish *Pagothenia bernacchii* (Ito *et al.*, 1995) and for crystals of the large 50S ribosomal subunit from the bacterium *Haloarcula marismortui* (Ban *et al.*, 1999). In both cases, the lengths of the *a* and *c* axes of the $P2_1$ crystals were indistinguishable from each other.

3.2. Comparison of MAD phases obtained with different software

The relative advantages of different software packages used for structure solution may not be of major importance for very high quality diffraction data, because all of them should be equally successful. However, if the data contain a high level of noise, it may be important to select a program that can best filter out the noise and give better initial electron-density maps. Here, five programs – *MADSYS* (Hendrickson, 1991), *MLPHARE* (Collaborative Computational Project, Number 4, 1994), *PHASES* (Furey & Swaminathan, 1995), *SHARP* (La Fortelle & Bricogne, 1999) and *SOLVE* (Terwilliger & Berendzen, 1999) – were used under the same resolution limits and similar refinement conditions to yield results suitable for direct comparisons (Table 3). The MAD phases calculated by these programs were subjected to the same solvent-flattening procedure using *DM* (Cowtan, 1994) from the *CCP*4 program suite. The quality of the electron-density maps was estimated by two theoretically equivalent methods. One method compared the MAD-phased electron-density maps with the map calculated from refined structural model using the program *OVERLAPMAP* from the *CCP*4 program suite. The correlation coefficients were calculated for all grid points in the maps. The other method calculated the correlation coefficients between the MAD-phased electron-density maps and each residue in the structural model using the program package *O*. In the latter case, only the grid points occupied by model atoms were compared.

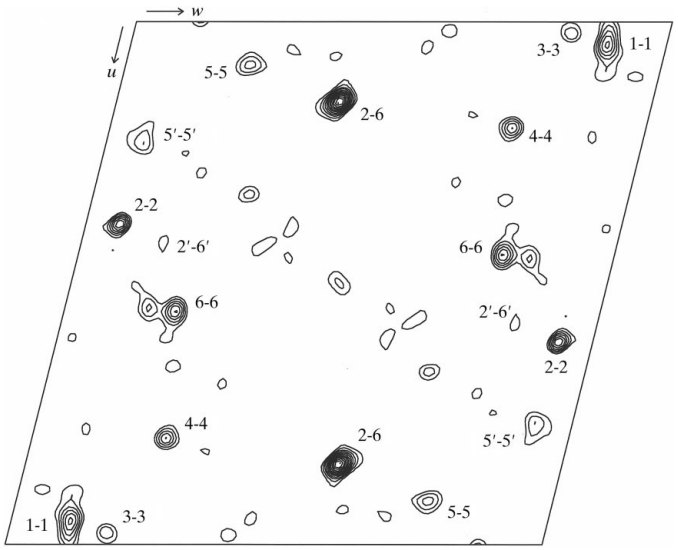

Figure 3
Harker section $v = \frac{1}{2}$ of the anomalous difference Patterson synthesis with the interpretation of the Se–Se vectors. The peaks are also listed in Table 3. Peaks marked with primes originate from the minor twinned component.

The phasing and map-quality statistics in Table 3 show little practical difference between the different approaches. Although the results obtained by using *MADSYS* with the detwinned and twinned data were slightly better for both the NSLS and APS data sets, these differences were marginal and indicated that, at least for these high-quality data sets, initial detwinning would not be crucial for the ultimate success of phasing. While the results obtained using *MADSYS* and *SOLVE* were very comparable for the twinned data, the map correlation coefficients after phasing with *SHARP* and *MLPHARE* were slightly lower and those obtained with *PHASES* were lower still. However, the phases calculated with all five programs yielded interpretable maps and the differences in the apparent results might reflect their performance under default conditions in the hands of users who have not had extensive experience with these packages, rather than major intrinsic advantages of one package over another.

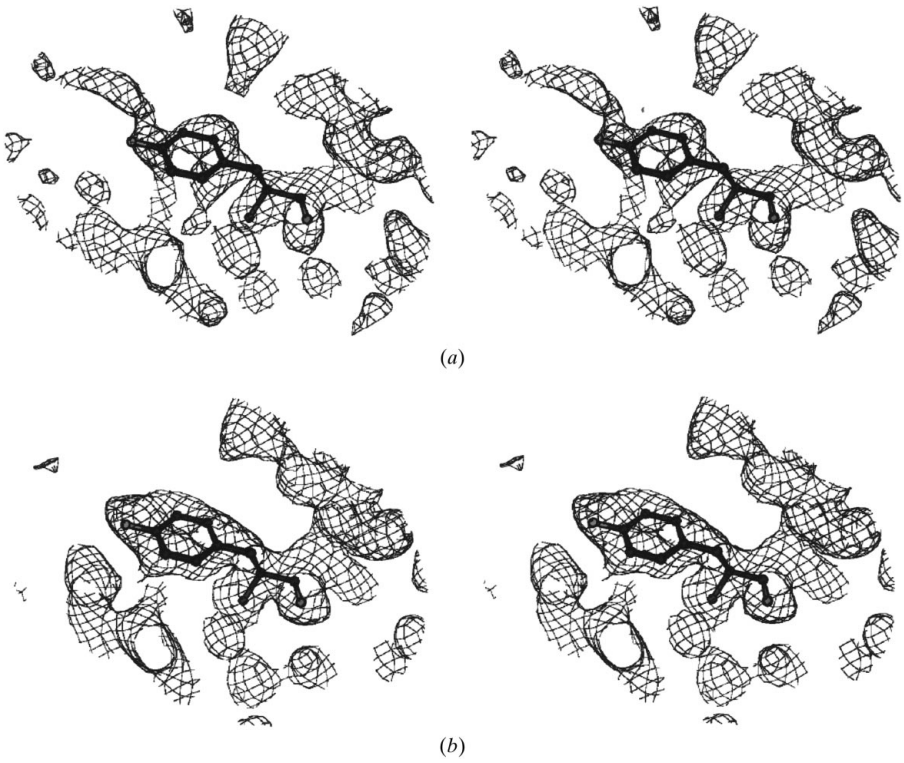

Figure 4
Comparison of the MAD-phased electron-density maps obtained after *MADSYS* and density modification from (*a*) twinned and (*b*) detwinned data. The map from the detwinned MAD data is better, with clearer densities around Tyr75.

3.3. Comparison of MAD-phased electron density

This new crystal structure of gpD was solved before the existence of twinning was realised. If the twinning problem had been noticed before the structure was solved, should the twinned MAD

data have been detwinned before phase calculation? In an attempt to answer this question and evaluate the quality of detwinned MAD data, both MAD data sets were detwinned and processed under the same conditions using *MADSYS*. The detwinning formula (equations 3 and 4) implies that if the errors of the two observed intensities from a twinned crystal are equal, then the errors of the intensities from the putative single crystals are increased by the factor $1/(1-2\alpha)$ as follows

$$\sigma_{s1} = [(1-\alpha)\sigma_{t1} + \alpha\sigma_{t2}]/(1-2\alpha), \quad (5)$$

$$\sigma_{s2} = [(1-\alpha)\sigma_{t2} + \alpha\sigma_{t2}]/(1-2\alpha), \quad (6)$$

where σ_{s1} and σ_{s2} are the errors of intensities estimated for the single crystal and σ_{t1} and σ_{t2} are the errors of the intensities actually observed for the twinned crystal. It should be noted that it is impossible to detwin the perfectly twinned data with α close to 0.5, since the errors are increased to infinity and the system of (3) and (4) is indeterminate. In our case, the twinning factor α is about 0.36; therefore, the errors are increased about 3.6 times. However, although errors are amplified by the detwinning process, our results show that the correlation coefficient between the MAD-phased electron-density maps and the maps calculated from the refined structural model is higher for the detwinned data than for the original twinned data. In other words, the quality of the MAD-phased electron-density maps from the detwinned data is higher than that of the original maps calculated from the twinned data. This can be clearly seen by comparing the electron densities around Tyr75 (Fig. 4). The density from twinned data is poor and is accompanied by a high level of ghost peaks near the tip of this side chain. On the other hand, the density from the detwinned data clearly shows the shape of the side chain of the tyrosine residue.

4. Conclusions

Although twinned crystals have been used before to solve protein structures by the molecular-replacement and isomorphous replacement methods, the gpD structure is to the best of our knowledge the first one to be solved from such crystals by MAD. Several conclusions can be made from our results. Firstly, a twinned crystal with a high twinning ratio may still prove useful for solving a new structure. If the data are collected at relatively high resolution with high quality and are properly detwinned, the calculated phases might still be accurate enough and the structure can be solved. Secondly, although different phase refinement and calculation programs can behave equally well with high-quality data, they may process twinned data slightly differently. Finally, although the detwinning process amplifies the errors in the intensities and reduces the signal-to-noise ratio, the detwinned data are still more accurate for phase calculation than twinned data.

The authors would like to thank Dr Mariusz Jaskólski for critical reading of the manuscript and Anne Arthur for editorial comments.

References

Ban, N., Nissen, P., Hansen, J., Capel, M., Moore, P. B. & Steitz, T. A. (1999). *Nature (London)*, **400**, 841–847.
Breyer, W. A., Kingston, R. L., Anderson, B. F. & Baker, E. N. (1999). *Acta Cryst.* D**55**, 129–138.
Brunger, A. T., Adams, P. D., Clore, G. M., DeLano, W. L., Gros, P., Grosse-Kunstleve, R. W., Jiang, J. S., Kuszewski, J., Nilges, M., Pannu, N. S., Read, R. J., Rice, L. M., Simonson, T. & Warren, G. L. (1998). *Acta Cryst.* D**54**, 905–921.
Collaborative Computational Project, Number 4 (1994). *Acta Cryst.* D**50**, 760–763.
Cowtan, K. D. (1994). *Jnt CCP4/ESF–EACBM Newslett. Protein Crystallogr.* **31**, 34–38.
French, S. & Wilson, K. (1978). *Acta Cryst.* A**34**, 517–525.
Furey, W. & Swaminathan, S. (1995). *Methods Enzymol.* **276**, 546–552.
Hendrickson, W. A. (1991). *Science*, **254**, 51–58.
Ito, N., Komiyama, N. H. & Fermi, G. (1995). *J. Mol. Biol.* **250**, 648–658.
La Fortelle, E. de & Bricogne, G. (1999). *Methods Enzymol.* **276**, 472–494.
Luecke, H., Richter, H. T. & Lanyi, J. K. (1998). *Science*, **280**, 1934–1937.
Otwinowski, Z. & Minor, W. (1997). *Methods Enzymol.* **276**, 307–326.
Rees, D. C. (1980). *Acta Cryst.* A**36**, 578–581.
Reynolds, R. A., Remington, S. J., Weaver, L. H., Fisher, R. G., Anderson, W. F., Ammon, H. L. & Matthews, B. W. (1985). *Acta Cryst.* B**41**, 139–147.
Sheldrick, G. M. & Schneider, T. R. (1997). *Methods Enzymol.* **277**, 319–343.
Terwilliger, T. C. & Berendzen, J. (1999). *Acta Cryst.* D**55**, 849–861.
Valegard, K., van Scheltinga, A. C., Lloyd, M. D., Hara, T., Ramaswamy, S., Perrakis, A., Thompson, A., Lee, H. J., Baldwin, J. E., Schofield, C. J., Hajdu, J. & Andersson, I. (1998). *Nature (London)*, **394**, 805–809.
Yang, F., Forrer, P., Dauter, Z., Conway, J. F., Cheng, N., Cerritelli, M. E., Steven, A. C., Plückthun, A. & Wlodawer, A. (2000). *Nature Struct. Biol.* **7**, 230–237.
Yeates, T. O. (1988). *Acta Cryst.* A**44**, 142–144.
Yeates, T. O. (1997). *Methods Enzymol.* **276**, 344–358.
Yeates, T. O. & Rees, D. C. (1987). *Acta Cryst.* A**43**, 30–36.